CR-152307

N79-29196

(NASA-CR-152307) AN IN-FLIGHT SIMULATOR INVESTIGATION OF ROLL AND YAW CONTROL POWER REQUIREMENTS FOR STOL APPROACH AND LANDING: DEVELOPMENT OF CAPABILITY AND PRELIMINARY RESULTS (Princeton Univ., N. J.) 44 p

Unclas

G3/08 34426

Princeton University

Department of
Mechanical and
Aerospace Engineering

MAE 1422

AN IN-FLIGHT SIMULATOR INVESTIGATION OF ROLL AND YAW CONTROL POWER REQUIREMENTS FOR STOL APPROACH AND LANDING: DEVELOPMENT OF CAPABILITY AND PRELIMINARY RESULTS

April 1979

Prepared for:

AMES RESEARCH CENTER
National Aeronautics and Space Administration
Moffett Field, California

Under Contract Number NAS2-7350

Prepared by:

D. R. Ellis
S. C. Raisinghani

FLIGHT RESEARCH LABORATORY
Department of Mechanical and Aerospace Engineering
Princeton University
Princeton, New Jersey 08544

TABLE OF CONTENTS

AN IN-FLIGHT SIMULATOR INVESTIGATION OF ROLL AND YAW CONTROL POWER REQUIREMENTS FOR STOL APPROACH AND LANDING: DEVELOPMENT OF CAPABILITY AND PRELIMINARY RESULTS

by

D. R. Ellis and S. C. Raisinghani

1. GENERAL INTRODUCTION

1.1 STOL FLYING QUALITIES RESEARCH

Although the general feasibility of STOL transports is widely accepted, utilizing any of several possible means of generating the needed lift at low speeds, the problem of how to configure the airplane and its control system to provide adequate handling qualities is still being actively pursued. Broadly speaking, the problem is one of providing the pilot with the means to suppress upsets and control the flight path accurately -- especially during the landing approach and touchdown -- under the adverse conditions which will frequently be encountered in STOL operations.

For future large STOL aircraft, unfortunately, the combination of slow approach speed and relatively high inertias results in poor flying qualities during landing approach. The reduction in dynamic pressure alone affects the basic stability characteristics of the aircraft and reduces its control effectiveness. The problem is further complicated by the presence of environmental disturbances; even moderate levels of turbulence, wind gradients, and steady wind have effects on the flight path and demand concentration and timely control inputs by the pilot. The slow, steep approach, if not inherently difficult in itself, at least may create problems in judging and controlling the flare and touchdown phases of the landing. At the same time, the requirements for accuracy

are extreme, since the runway may be short and elevated or surrounded by obstacles, and visual cues may be deficient during night or bad weather operations.

These problem areas have been identified and discussed for some time within the research community and the need for further work is clearly indicated (Ref. 1 and 2, for example). Some of this research is already underway, using advanced analytical techniques and ground-based simulators. However, even the most enlightened analysis is usually incapable of fully describing the complex piloting operations, and even the most advanced ground-based simulators may have deficiencies in motion capability and visual cues for landing; thus, it is desirable to confirm the results obtained from those sources in flight before they are fully accepted for design use. Complete confidence will only come with the flying of actual STOL transports, of course, but an interim approach is to use in-flight STOL simulation to validate, and possibly expand, the knowledge gained in other ways. The investigation described in this report deals with such a program of in-flight STOL approach and landing simulation utilizing one of Princeton's Variable-Response Research Aircraft. This machine is capable of simulating a broad range of STOL vehicle response characteristics, with correct representation of task and disturbances; it is described in some detail in Appendix A.

1.2 PROGRAM OBJECTIVES

It is apparent from recent efforts in STOL simulation that most of the outstanding handling problems are those related to path control rather than stabilization in the small perturbation sense. Quite a bit is known about desirable levels of rotary damping and static stability (Ref. 3-6), and it seems likely that any production vehicle will be equipped with reliable stability augmentation sufficient to provide at least minimum acceptable levels in those areas. On the other hand, we appear to be just now gaining an understanding of how the various vehicle parameters influence path and speed control

during approach and touchdown. Furthermore, the question of what constitutes adequate control power to satisfy combined trim, maneuvering, and gust suppression requirements is, in most respects, without a definitive answer.

The broad objective of the program is to investigate through in-flight simulation some important aspects of the lateral-directional control power requirements during the STOL approach and landing in the presence of external disturbances. This includes:

- Investigation of the roll- and yaw-power requirement for approach-and-landing flight phases and, in particular, to determine the desirable and acceptable control power levels in presence of crosswind and/or turbulence, considering both sideslip and crabbed approaches.
- To evaluate lateral-directional parameters which may affect the control power requirements, especially in presence of a crosswind.
- To investigate the various roll and yaw response criteria with a view to extending and updating those suggested in Ref. 1.

2. TECHNICAL DISCUSSION

2.1 CONTROL POWER REQUIREMENTS

The STOL transport designer is faced with the problem of providing adequate control power for large, high-inertia vehicles flown at speeds so low that conventionally-sized aerodynamic surfaces are inadequate. Since providing excess control power will result in penalties in terms of power and weight, it is important to determine the minimum required to perform critical tasks. Control power demands are most likely to be highest during the approach and landing, since the pilot must be able to combine approach maneuvering (localizer tracking and runway offset) with gust upset suppression and crosswind correction. In addition to such mission and task dependence, the control power requirements will be influenced by the basic dynamic characteristics of the airplane. Low dihedral effect, for example, will lessen demands on roll control power in sideslipping crosswind corrections and in turbulence. Low directional stability will favor easy sideslip entry, small steady rudder deflections for intentional sideslips, and small yaw response to turbulence. Either very large or very small levels of rotary damping will lead to increased demands on control power in the first case to overcome sluggish response, in the second to cope with motion overshoots.

The present program is directed toward this question and represents development of a facility to determine the minimum lateral-directional control power for desirable and acceptable levels of handling qualities for the STOL landing approach task in a variety of simulated atmospheric disturbance conditions for a range of lateral-directional response characteristics.

2.2 CROSSWIND LANDINGS AND THEIR SIMULATION

STOL aircraft are in some respects more adversely affected by atmospheric disturbances than CTOL aircraft -- because of reduced approach speed the steady wind component may be as much as 40 to 50 percent of the airspeed. Furthermore, the location of STOL landing sites may be in areas surrounded by trees or buildings which expose the STOL aircraft to severe atmospheric disturbances. Also, the choice of landing strip (in terms of direction) may be limited. Thus, it seems likely that STOL aircraft will perform crosswind landings more often than CTOL airplanes do.

Two different techniques normally are used in crosswind landings: the wing-low (or sideslip) approach and the crabbing approach. In the sideslip approach, the upwind wing is lowered to produce a lift component equal to the crosswind force, and opposite rudder is applied to keep the airplane's longitudinal axis aligned with the runway heading. In the crabbing approach, the aircraft is turned in the direction of the crosswind to a degree sufficient to prevent the drifting of the airplane with respect to the ground. Because of the lack of sideslip, the aileron and rudder controls are essentially neutral, and the wings are level. The heading is aligned with the runway just before the touchdown. In practice, the two techniques are often combined (that is, a crabbing approach transitioning to a wing-low sideslip shortly before touchdown).

To simulate crosswinds, Princeton's 6-degree-of-freedom Variable-Response Research Aircraft (Navion 91566) has been modified suitably and is shown in Fig. 2-1. Two servo-driven surfaces (referred to hereinafter as side-force surfaces) have been installed on each wing (see Fig. 2-2). These are used to balance all or part of the side-force developed when the Navion is flown in a steady sideslip, thereby presenting the pilot with the impression of flying a crabbing crosswind

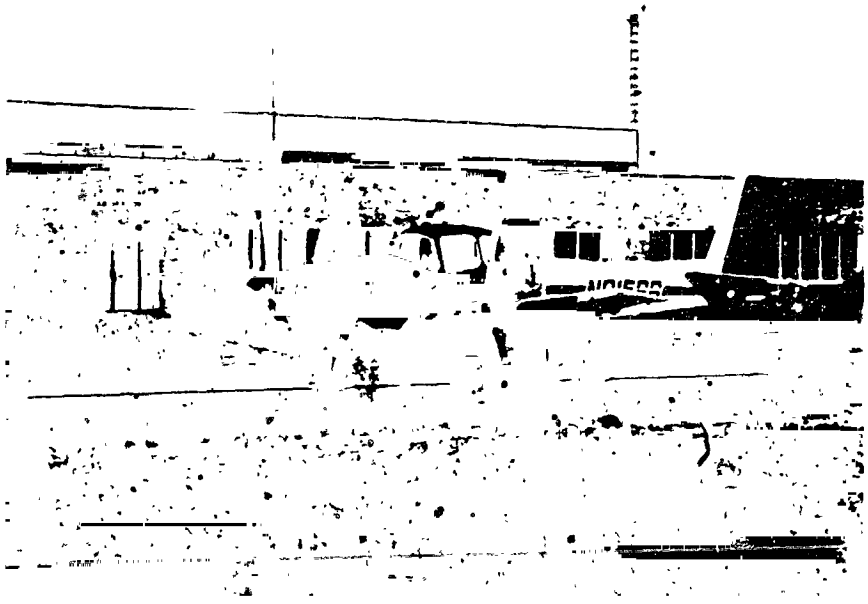

Figure 2-1. Variable-Response Research Aircraft (VRA).

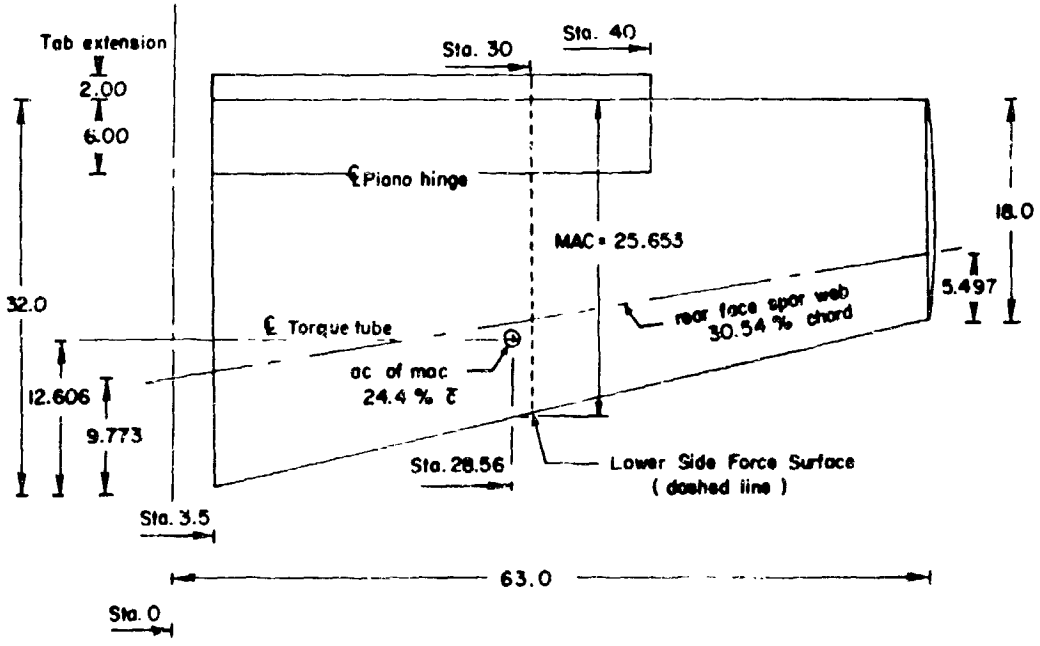

Figure 2-2. Side Force Control Surfaces.

correction. The side-force surfaces are capable of generating ±0.25-g peak lateral acceleration at 75-kt airspeed and a steady sideslip of nearly ±15 deg, with some margin left for simulating dynamics (e.g., to reduce Y_β). A 15-kt crosswind component for a flight speed of 75-kt may be comfortably simulated. At higher sideslip angles, flow separation on the side-force surfaces leads to buffeting. For safety considerations, the crosswind simulation is restricted to 20-kt at the flight speed of 75-kt. Some details of the flight experiments flown to define side-force authority are given in Appendix B.

2.3 TURBULENCE SIMULATION

The level of control power acceptable for a no-turbulence condition may not be adequate when landing in the presence of turbulence, and any simulation should include a reasonable realistic representation of such disturbances. Each of the components of a turbulent atmospheric field produces aerodynamic loads on the airplane leading to excitation of airplane motions, the response depending on the stability derivatives of the airplane. This is simulated with the Navion by means of appropriately scaled and filtered tape recorded signals introduced into the control system. Background and details of this turbulence simulation scheme are given in Ref. 7 and 8.

3. DESCRIPTION OF EXPERIMENT

3.1 IN-FLIGHT SIMULATOR

The flight evaluation program was conducted in the Princeton Variable-Response Research Aircraft, shown in Fig. 3-1 and described in detail in Appendix A. Some of the important features of this airplane relevant to the present investigation are as follows:

- Aerodynamic forces and moments are independently variable. This is done by electro-hydraulic actuation of throttle, direct lift flaps, elevator, aileron, rudder and side-force surfaces.
- There is provision for changing, in flight, the maximum roll and yaw control power through the use of electronic limiters; control sensitivity ($rad/sec^2/in$) is variable independent of maximum control power.
- Separate "fly-by-wire" cockpit controls are used by the evaluation pilot. The evaluation cockpit has a standard IFR instrument display and a sideslip (β) meter.
- Telemetry is used to acquire motion parameters (linear accelerations, angular rates, attitude and heading), control inputs, control surface positions, and performance measures such as localizer and glide slope deviation. The telemetry system has 43-channel capacity. Telemetry data and voice comments are tape recorded.

3.2 CROSSWIND SIMULATION

Servo-driven side-force surfaces provide the capability for simulation of crosswinds (the airplane is flown in a steady sideslip with just enough side-force surface deflection to cancel the side-force which develops through Y_β and $Y_{\delta r}$: the resulting wings-level, ball-centered sideslip appears to the pilot as a "crabbing" crosswind

correction). The side-force surface authority, determined through the steady sideslip experiments discussed in Appendix B may be expressed as;

$$\frac{Y_{\delta y}}{V} = \frac{1}{mV}\frac{\partial Y}{\partial \delta y} = 0.25 \text{ sec}^{-1} \text{ rad}^{-1} \quad \text{at } V = 75 \text{ kt.}$$

The following ranges of variables are considered:

- Maximum lateral acceleration $\simeq \pm 0.25$ g @ V = 75 kt.
- Maximum steady sideslip capability $\simeq \pm 15^{o}$
- Maximum crosswind simulation at flight speed of 75 kt ~ 20 kt

It should be pointed out here that the limitation on the sideslip capability (or maximum crosswind simulation) arises due to flow separation and the resulting buffeting at large side-force surface deflection; the surface deflection itself is not limited. This may be seen in Fig. 3-1, which shows the crosswind simulated as a function of side-force surface deflection. Furthermore, the amount of side-force surface deflection needed for a specific crosswind simulation is also dependent on the value of Y_{β}, since $Y_{\beta}\beta \doteq Y_{\delta y}\delta y$ (neglecting $Y_{\delta r}$), where $\beta = v_{cw}/V$ with v_{cw} denoting the crosswind, and V denoting the flight speed. Thus, we may write,

$$\delta y = Y_{\beta}/Y_{\delta y} \cdot v_{cw}/V$$

To generate pure side-force when the side-force surface is deflected, interconnects were provided between the side-force surface deflection and ailerons and rudder. By analog matching, it was possible to find the correct gain settings for crossfeed such that the rolling moment due to side-force surface deflection, $L_{\delta y}$, and yawing moment due to side-force surface, $N_{\delta y}$, are both zero.

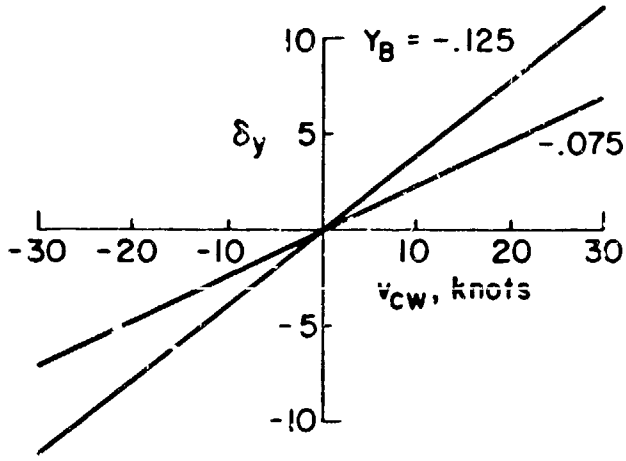

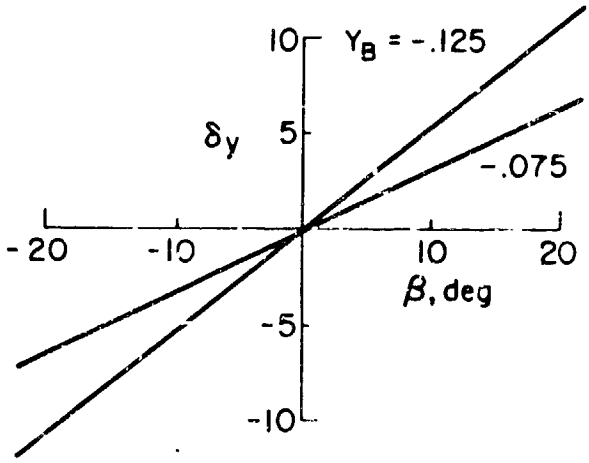

Figure 3-1. Simulation of Crosswind.

3.3 TURBULENCE SIMULATION

The model of the turbulence-induced aerodynamic disturbances used in the present investigation is described in Ref. 7 and 8. A brief account of the model is included here for completeness. The contribution of the longitudinal (u_g) velocity component to the airplane's gust response is assumed to be negligible compared to the lateral (v_g) and vertical (w_g) components. The lateral (v_g) velocity component is taken to be constant along the x and z axes, whereas for the vertical (v_w) velocity component, both $w_{g\ long}$, the component of w_g that is constant along y axis, and $w_{g\ lat}$, accounting for the spanwise gradient of the vertical gust, are included. Prefiltered gaussian white noise is recorded on three channels of the tape to represent the three uncorrelated random gust components corresponding to $w_{g\ long}$, $w_{g\ lat}$ and v_g. These signals are passed through filter circuitry in which the desired spectral characteristics are achieved by varying the filter break frequency according to the simulation model. By adjusting the gains, it is possible to match the required rms gust velocity and aerodynamic stability in the separate axes. Separation of the tail surface from the wing is simulated by using a first-order Padé time delay approximation. Finally, the filtered signals are fed to their respective control surface servos.

Gust intensities of 5.5 ft/sec rms were simulated for all the three gust components, namely, $w_{g\ long}$, $w_{g\ lat}$, and $v_{g\ lat}$. According to Ref. 9, the probability of equaling or exceeding this rms gust velocity once the turbulence is encountered is about ten percent.

3.4 TEST CONFIGURATIONS

Table 3-1 below lists designators (such as X-15), derivatives, and modal characteristics for a set of suitable test configurations.

TABLE 3-1

SIMULATED STOL AIRPLANE CONFIGURATIONS

Y_β	-0.075				-0.125	
ζ_d	0.4		0.1		0.1	
ω_d	1.3	0.8	1.3	0.8	1.3	0.8
N_p=-0.1	X-15	X-7	X-6	X-3	X-20	X-18
N_p=-0.3	X-13	X-9	X-4	X-1	X-22	X-16

Parameters Common to all Configurations:

$\tau_r = 0.5$ $\quad L_r = 0.75$ $\quad L_\beta = -0.4$

τ_s, Variable, neutral or slightly unstable $\quad N_{\delta a} = 0$

$V_o = 75$ kt $\quad L_{\delta r} = 0$

Discussion of Configurations - The influence of the Dutch roll characteristic on the lateral-directional handling qualities has been amply demonstrated in the past for all categories of airplanes. Dutch roll frequency, ω_d, and damping, ζ_d, strongly affect the piloting technique employed for the landing-and-approach phase of the flight. As reported in Ref. 3, the combination of ζ_d and ω_d has a direct effect on the pilot's ability to handle a crosswind approach -- specifically, low damping ratio does not present serious problems at high Dutch

roll frequency but becomes a major problem at low frequency. Therefore, four basic Dutch roll variations were chosen for study:

- High ζ_d (= 0.4) and high ω_d (1.3 rad/sec) (Highly augmented)
- High ζ_d (= 0.4) and low ω_d (0.8 rad/sec)
- Low ζ_d (= 0.1) and high ω_d (1.3 rad/sec)
- Low ζ_d (= 0.1) and low ω_d (0.8 rad/sec) (No augmentation)

The roll mode time constant, τ_r, characterizes the roll response of the airplane to the aileron input. Past experience (e.g. Ref. 3) indicates that roll mode time constants as long as one second do not adversely affect the pilot's control in a crosswind. Since most projected STOL transport airplanes will have wings of reasonably high aspect ratio, and/or provision for artificial roll damping, it seemed reasonable to keep τ_r constant for all the evaluation configurations of the present investigation. The value chosen was a nominal τ_r = 0.5 sec.

The spiral mode usually is not considered important for the landing approach phase of the flight and is, in most studies, fixed at a neutral value (e.g., Ref. 10). However, a neutral spiral mode will require $L_\beta N_r = N_\beta L_r$; thus, moderate to high L_β and N_r will result in large L_r which may not be a representative value for a STOL airplane. Relaxing the requirement for a neutral spiral mode permits setting L_r at a representative value. The computational method used involves setting the coefficients of the characteristic quartic of the homogeneous lateral-directional equations equal to the coefficients of the product of the roll mode, spiral mode, and Dutch roll mode; values of Y_β, L_β, L_r, N_p, ω_d, ζ_d, and τ_r are selected, and $1/\tau_s$, N_β, N_r, and L_p are solved for.

The magnitude of the side-force derivative, Y_β , may be an important factor for crosswind landings of STOL airplanes, since in a sideslip

approach, the bank angle required is directly proportional to its value. It was decided to try two variations, a typical value of $Y_\beta = -0.125$ and a smaller value of $Y_\beta = -0.0$[illegible].

The cross derivative N_p (yaw due to roll) also will affect the piloting technique and rudder control power required in side-slip approaches and landings. A typical value of $N_p = -0.1$ was picked for most of the evaluation configurations, with a larger value of $N_p = -0.3$ chosen to isolate the effect of large adverse yaw due to roll on the pilot task and control power requirements.

The dihedral stability derivative L_β (= -0.4) and roll-due to-yaw derivative L_r (= .75) were held constant. Although L_β does, in general, have an important influence on roll control power requirements, values for non-swept wing STOL transports are typically of the order shown, and it was decided not to include additional variations in this study. However, it is a factor deserving further consideration.

The cross control derivatives -- yaw due to roll control $N_{\delta a}$, and roll due to rudder, $L_{\delta r}$ --both were set at zero,as might be done with interconnects on an actual airplane. The derivative $N_{\delta a}$ is well known (Refs. 10 and 11, for example) to influence control of bank angle, but this effect is small if the level of L_β is low, as it is here. Control coordination and yaw control power will be influenced by the level and sign of $N_{\delta a}$, but it was felt that zero levels would provide a good baseline.

Roll and yaw control sensitivity -- aileron and rudder deflection per unit control stick or pedal movement --were selected by the pilot by simply varying the appropriate gain potentiomenter. To restrict the number of variables, it was decided that the pilot would be free to select the most desirable level of control sensitivity

during the familiarization flights; once selected, it would be held at that value throughout the test sequence.

The available control power is varied by using cockpit-adjustable electronic limiters which operate on control signals to the aileron and rudder servos in such a way that the commanded surface deflections are restricted (Fig. 3-2). The stick and rudder pedals retain their normal mechanical range.

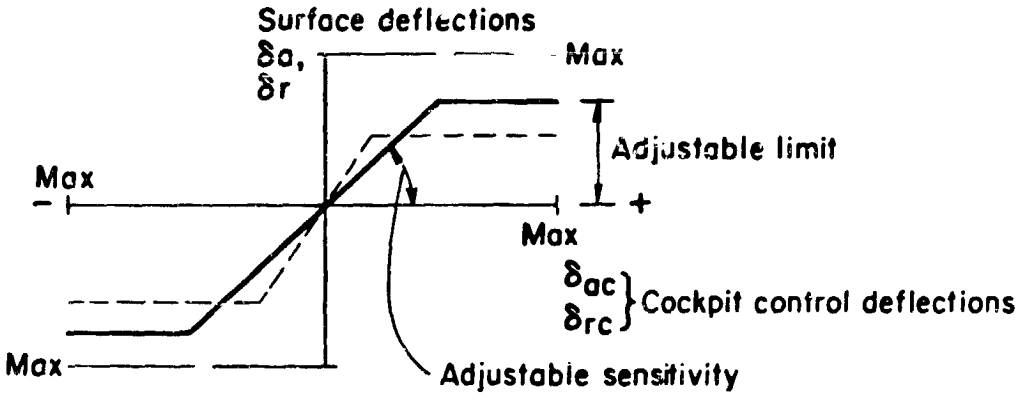

Figure 3-2. Aileron and Rudder Limiter Scheme

Since lateral-directional handling qualities during approach and landing were the primary concern, the longitudinal characteristics were held constant at generally satisfactory levels for all the STOL configurations evaluated in the present program. The important stability derivatives are listed below (Nomenclature of Ref. 12):

$$\frac{Z_c}{V} = -0.8 \text{ ft/sec}^2/\text{rad} \qquad M_{\dot{\theta}} = -1.7$$

$$M_\alpha = -0.204 \text{ rad/sec}^2/\text{rad} \qquad M_{\dot{\alpha}} = -0.82$$

$$M_{\delta e} = -8.7 \text{ rad/sec}^2/\text{rad} \qquad M_V = 0$$

$$(D_V - T_V) = 0.16$$

$$(D_\alpha - g) = -12$$

3.5 EVALUATION PROCEDURES

The piloting task consisted of an IFR final approach transitioning to visual flight at 200-ft AGL, a lateral offset maneuver, and a flare and touchdown using either wing-low or decrab crosswind correction. The flight profile of a typical run is shown in Figure 3-3. The sequence of events is as follows:

- Familiarization with the configuration
  a. Adjust roll and yaw control sensitivities to desirable levels.
  b. Check trimmability and perform small amplitude maneuvers to find capability of performing precise changes in bank angle and heading.
- Intercept localizer at about 1.25 nm from the landing field and at about 800 ft altitude (this results in a lateral offset of approximately 200-ft to the right of the runway due to the location of Talar system), stabilize the airplane at 75 kt, and turn on simulated crosswind and turbulence as may be appropriate for the particular configuration being tested. Fly down to 200-ft altitude following the ILS glide slope of 6 deg.
- At 200-ft altitude, transition to a VFR landing approach, making an "S" turn maneuver to align the flight path with the runway centerline.
- Use wing-down "sideslipping" or crabbed short final approach and land the airplane on (or as close as possible) to the runway centerline.

The evaluation pilot was asked to comment upon and rate (using the familiar Cooper-Harper scale) each run, separating the straight-in, offset, and landing phases if necessary.

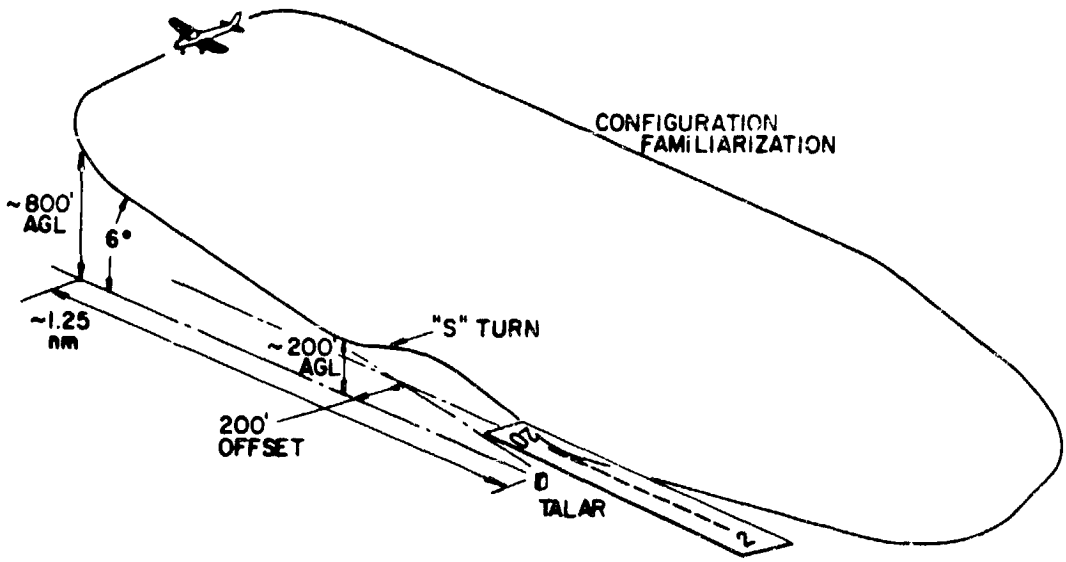

Figure 3-3. Evaluation Flight Pattern

4. RESULTS AND DISCUSSION

4.1 GENERAL REMARKS

It should be noted at the outset that the results discussed herein are of a preliminary nature, based on a limited number of runs by only one evaluation pilot, albeit with extensive STOL simulation experience. However, enough testing was completed to indicate certain trends, and the suitability of the in-flight simulator for crosswind landing research was demonstrated.

In the course of the testing, data were gathered which bear on the objectives of exploring roll and yaw control power requirements for the croswwind landing maneuver, and on the effects of variations in yaw due to roll rate and Dutch roll damping ratio. The testing was too limited to be able to judge various response criteria.

4.2 CONFIGURATIONS TESTED

The discussion in this section will focus on three of the configurations listed in Table 3-1 of Section 3, namely X-15, X-13, and X-4, with the first two receiving the bulk of the attention. The only difference between X-15 and X-13 is in the level of yaw due to roll rate (N_p = -0.1 and -0.3, respectively); X-4 is the same as X-13 except for a smaller Dutch roll damping ratio (ζ_d = 0.1 rather than 0.4).

Preliminary trials with clearly adequate control sensitivity and control power settings ($L_{\delta a} \geq 0.4$, $N_{\delta r} \geq 0.3$; $L_{\delta a}\delta a_{max} \geq 1.2$, $N_{\delta r}\delta r_{max} \geq 0.7$) confirmed satisfactory lateral-directional behavior for all three airplanes on $\gamma_A = 6^o$, straight-in, no crosswind MLS

approaches and landings, meriting pilot ratings of 3.0 for X-15 and X-13 and 3.5 for the more lightly damped X-4. Longitudinal characteristics were felt to be representative of a well-augmented STOL transport which could be flared to a low sink rate touchdown from the 75 kt approach without the need for throttle advance.

4.3 EVALUATION TASK

Before considering particular results, it is well to have in mind the following overall observations on the relative difficulty and importance of the various parts of the evaluation:

- The MLS-tracking portion of the approach was straight forward and relatively easy, even with low control power, due to the small-amplitude corrections required (the presence of simulated wind shear might change this, however).

- The offset maneuver proved to be relatively difficult due to its amplitude (200 ft) and close proximity to the runway threshold. After transition to visual flight at a 200-ft altitude, the maneuver had to be initiated without delay in order to be completed in time for a short straight final approach before flare and touchdown. In retrospect, this magnitude of offset may be too demanding of roll control power, and undoubtedly influenced these preliminary findings.

- The touchdown phase could or could not be the most critical during any given run, depending on the amount of simulated crosswind, the correction technique (decrab or wing-low, or combination) and, of course, the amount of control power available.

- As a broad generalization, the offset maneuver was the most critical of the three evaluation phases, especially when roll control power was low; the touchdown out of a decrab maneuver was critical with low yaw control power.

4.4 PILOT RATING TRENDS

Roll Control Sensitivity

Pilot rating trends with roll control sensitivity are indicated in Table 4-1, which lists a series of six landings with configuration X-15 in various conditions of simulated wind and with both wing-low and decrab landing techniques. As seen from the table, the first three trials used $L_{\delta a} = 0.43$, and the last three used progressively lower values ending at $L_{\delta a} = 0.17$. Rudder power and sensitivity were satisfactory.

The trend is clearly for the rating to degrade as sensitivity is lowered, although an anomaly appears in the area of control usage -- a smaller percentage of available control power being used at the lower sensitivities than at the higher ones. These are peak measurements, occurring in the rollout from the offset maneuver; it appears that the pilot preferred to make relatively brief, large inputs with the high sensitivity and longer, small inputs (with more lead) with lower effectiveness. Additional data from more pilots are obviously needed to confirm this.

Roll Control Power

Pilot rating trends with roll control power are shown in Fig.4-1 for various approach and wind conditions. The data represent the maximum used by the pilot on a given run, this almost invariably occurring on the rollout from the sidestep maneuver if that was featured on the approach. It should be noted that the lowest "maximum available" control power used in these runs was $L_{\delta a}\delta a_{max} = 0.7$, and was sometimes higher, so the individual points do not necessarily represent cases where the pilot had the roll control on the stops; this is a fairly important point since some pilots object strongly to running out of control margin even if the amount available is just sufficient for the task. (The

TABLE 4-1

Pilot Rating Trends as a Function of Roll Sensitivity

Configuration X-15

Run	$L_{\delta a}$	Maximum Roll Power Use, % Left	Right	Type of Approach, Technique, Wind	Rating and Comment
1	.43	33	70	Straight-in; No Crosswind	3.0; Sensitivity and Power ($L_{\delta a}\delta a_{max}$=1.0) Adequate
2	.43	66	83	Sidestep, Wing Low; 10 kt Left	3.0; Adequate for Sidestep
3	.43	20	100	Sidestep, Decrab; 10 kt Left	3.35; Based on Sidestep Roll-out, momentary full control; δ_r OK.
4	.34	64	100	Sidestep Decrab; 10 kt Left	4.0
5	.25	51	66	Sidestep Wing Low; 10 kt Left	4.0; Still Adequate for Side-step and Crosswind Correstion.
6	.17	69	51	Sidestep Wing Low; 10 kt Left	4.5; Still Adequate

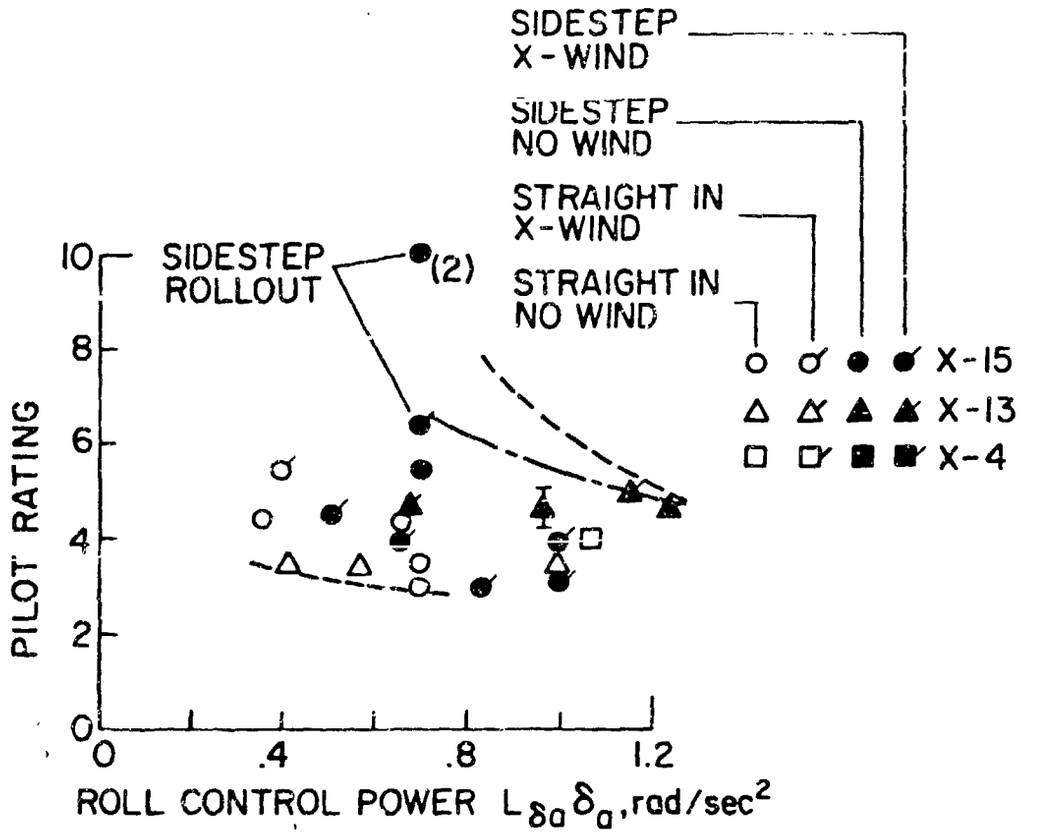

Figure 4-1. Pilot Rating Trends as a Function of Roll Control Power.

outlook here was that although desirable, a margin was not necessary; however, the increase in workload due to the need for greater anticipation and planning was accounted for in the rating).

The data indicate that control power as low as $L_{\delta a}\delta a_{max} \approx 0.25 - 0.3$ (assuming a 0.2 sec ramp control input, this would permit 30° of bank in about 4 sec) might be rated as satisfactory for a basically well-behaving airplane on a straight-in, no-wind, no-turbulence approach. On the other hand, it appears that clearly adequate roll control for crosswinds, sidestep maneuvers and less than optimum piloting technique requires something more in the neighborhood of $L_{\delta a}\delta a_{max} = 1.0$ (30° of bank in about 1.8 sec). There were two occurrences of missed approaches (rated 10) due to inability to roll out quickly enough - even with full control input-to complete the side-step without badly overshooting the runway; poor planning or positioning while rolling in or out of the maneuver probably was the cause, but there was no margin available for such errors in technique.

Yaw Control Power

Trends of pilot rating with yaw control power are shown in Fig. 4-2 for crosswind and no-crosswind conditions. As might be expected, in no-crosswind conditions very little rudder power is needed with X-15 and X-13 which are well-damped ($\zeta_d = 0.4$) and have very little Dutch roll excitation from roll control inputs; in fact, many acceptable feet-on-the-floor approaches in both airplanes can be made in those circumstances.

Mainly as a result of the basic configuration (low directional stability and low roll/yaw coupling from small values of L_β, N_p, and $N_{\delta a}$), wing-low crosswind corrections put small demands on rudder power, and the decrab maneuver was the critical one.[1] These preliminary data indicate that the area of clearly adequate control power lies above $N_{\delta r}\delta r_{max} = 0.4$. With the particular $N_{\delta r}\delta r_{max} = 0.3$ case rated 10, a late start on the decrab resulted in the airplane reaching the touchdown zone with an unacceptably large crab angle which could not be readily "kicked out"; although successful no-drift touchdowns were often made with less rudder use, there was little margin for error.

Effects of N_p

As indicated in Table 3-1, configurations X-15 and X-13 were essentially the same except for the value of the yaw due to roll derivative, N_p (-0.1 for X-15, -0.3 for X-13), which caused configuration X-13 to yaw more on uncoordinated turn entries, and to have more Dutch roll excitation on entry to wing-low crosswind correction sideslips.

[1] It might be noted that due to low dihedral all configuations flown appeared to the pilot to be decoupled, with the Dutch roll being essentially a wings-level yawing oscillation. The decrab maneuver thus was simple to perform requiring only a properly timed heading change with the rudder.

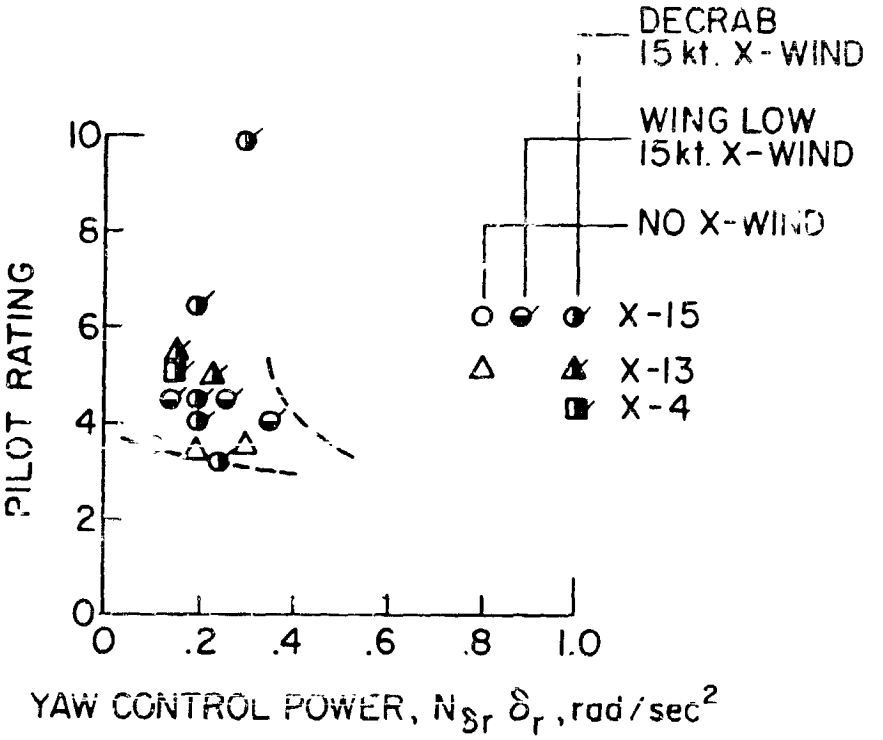

Figure 4-2. Pilot Rating Trends as a Function of Yaw Control Power.

The data in Table 4-2 are taken from selected runs with comparable (and satisfactory) levels of $L_{\delta a}$ and $N_{\delta r}$.

Although there were no specific comments on problems with rudder usage, and the peak control inputs are of about the same level, the ratings tend to indicate a higher workload with X-13. Again, more data are needed to confirm this.

Effects of Dutch Roll Damping

Configuration X-4 was the same as X-13 in its characteristics except for a lower Dutch roll damping ratio (ζ_d = 0.4 for X-13, 0.1 for X-4). In runs with the same conditions of crosswind and technique,

X-4 was consistently degraded one-half unit in pilot rating compared to X-13, and was described as "lightly damped" in the commentary. With favorable control power and sensitivity, however, this level of damping in itself would not appear to present piloting problems.

TABLE 4-2

Pilot Ratings for Two Levels of N_p

Configuration X-15 : $N_p = -0.1$

Configuration X-13 : $N_p = -0.3$

Flight Condition	Maximum Roll Power Used		Maximum Yaw Power Used		Pilot Rating	
	X-15	X-13	X-15	X-13	X-15	X-13
Visual Sidestep, No Crosswind	+.69 -.33	+.96 -.75	+.31 -0.10	+.12 -.11	3.0	4.5-5.0
Left Crosswind 10 kt, Wing-Low Correction	+.83 -.66	+.75 -1.22	+.23 -.14	+.086 -.20	3.0	4.5-5.0
Left Crosswind 15 kt, Wing-Low Correction	+1.25 -0.47	+.97 -1.15	+.23 -.21	+.093 -.186	3.0	5.0

5. CONCLUSIONS

The following conclusions are based on a limited sampling of simulated STOL transport configurations flown to touchdown out of 6^{o}, 75 kt MLS approaches, usually with a sidestep maneuver:

1. The utility of the variable response airplane with side force surfaces in this simulation mode - STOL transport crosswind operations - was successfully demonstrated. All of the planned functions except wind gradient with altitude were demonstrated.

2. The roll control power results appear to be quite sensitive to the geometry of the approach, particularly the sidestep maneuver; in this case, the low initiation altitude of 200 ft AGL and 200 ft offset from the runway centerline called for prompt and correct pilot action and tended to favor high control power.

3. Based on these preliminary trials with moderate roll damping (τ_r = 0.5 sec), roll control power as low as $L_{\delta a}\delta a_{max}$ = 0.25 rad/sec^2 may be acceptable for straight-in approach, no-crosswind operations; in order to have clearly acceptable control in conditions involving moderate crosswind and maneuvering, $L_{\delta a}\delta a_{max} \geq 1.0$ rad/sec^2 is needed. This corresponds to a capability to bank 30^{o} in about 4 sec in the first case and about 1.8 sec in the second.

4. Although zero rudder power is acceptable in some non-maneuvering cases, normal operations with crosswinds appear to require $N_{\delta r}\delta r_{max} \geq 0.4$ rad/sec^2.

5. Significant degradation in pilot rating may be obtained by changing the value of yaw due to roll rate from N_p = -0.1 to -0.3, or by lowering Dutch roll damping ratio from ζ_d = 0.4 to 0.1; however, given adequate control power and sensitivity, the basic configuration under study was not seriously compromised by either change.

APPENDIX A

VARIABLE-RESPONSE RESEARCH AIRCRAFT

The Princeton Variable-Response Research Aircraft is based upon a modified Ryan Navion light airplane. The most important airframe modifications made are as follows:

- The flap hinging and actuation have been changed to permit upward as well as downward deflection of the flap and thus increase lift modulation capability.
- The rudder area has been increased by approximately 50 percent to improve yaw control power.
- The normal Navion main landing gear struts have been replaced by those from a Camair twin (Navion conversion) to permit landing sink rates as high as 12.5 ft/sec.
- Side-force surfaces are installed on each wing. The surface used is shown in Figure 2-2. The span of the side-force surface below the wing was determined by the maximum height which would allow 10 deg of bank with the landing gear shock strut compressed. The spanwise and chordwise location of the surfaces was primarily governed by the considerations of structural strength and ease of installation.

Variable Response Control System

The most basic modification of the airplane is the provision of a "fly-by-wire" control system. Fast-acting hydraulic servos are used to drive the ailerons, rudder, elevator, flaps, and side-force surfaces. Signals from the evaluation pilot's controls and sensors measuring the flight variables are appropriately processed and summed, and they provide the net signal for each servo-actuator. The magnitude scaling of each control or sensor signal is done by a separate potentiometer in the airplane; thus, by properly varying the potenticmeter

settings, the dynamic response characteristics of the basic Navion may be changed in a desired manner in flight.

Several interconnects are provided to achieve single-degree-of-freedom control. An interconnect between flap and elevator can be so adjusted that the flap deflection will produce only incremental lift, the pitching moment due to flap being cancelled by the elevator deflection. Similarly, a coupling of side-force surfaces with ailerons and rudder is used to eliminate rolling and yawing moments due to side-force surface delection, so that the side-force surfaces may act as pure side-force generators. It is thus possible to achieve independent control over the three angular and three linear degrees of freedom.

Cockpit and Evaluation Pilot Controls

The instrument panel and controls are shown in Figure A-1. The left seat is occupied by the safety pilot, who operates the normal Navion wheel and rudder pedals and power plant controls. An overhead panel contains gain potentiometer and switches which can be operated by the safety pilot to vary the stability and control parameters for simulating the desired configuration. A meter (see Figure A-1) is provided to indicate the position of the side-force surfaces. Controls are located just below the meter for operating side-force surfaces. The safety-pilot uses the side-force control to balance the airplane for a straight, level-flight condition and then with a separate control sets the side force surfaces according to a calibrated scale for any steady sideslip condition, such as a simulated crosswind. Upon system disengage, the surfaces return to the pre-set trim deflection.

The gain potentiometers limiting the maximum deflection of ailerons and rudder are located on two hand-held boxes and can be operated by the safety pilot to vary the maximum roll and yaw power available to the evaluation pilot. The control motion gradients--surface

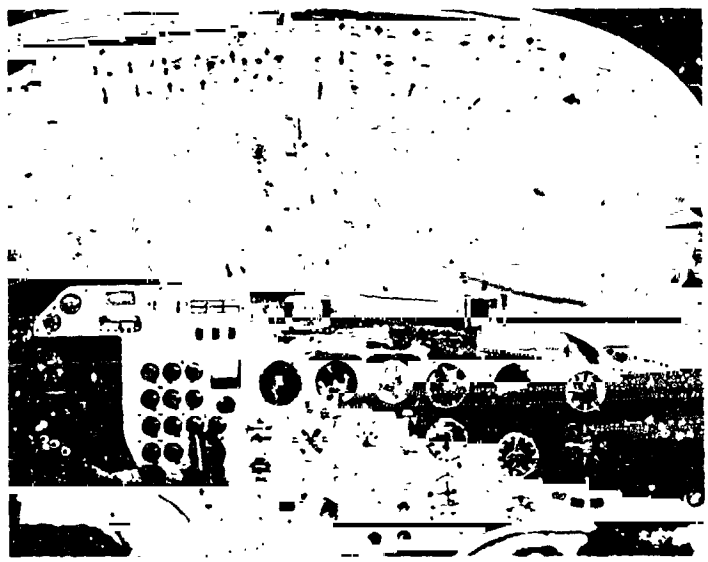

Figure A-1. VRA Instrument Panel.

deflection per inch movement of control -- can be varied by changing the gain potentiometers located on the overhead panel on safety pilot's side. The gain potentiometers for turbulence simulation are located on the lower central panel and can be adjusted by the safety pilot.

The evaluation pilot is seated on the right and is provided with a standard flight instrument layout and conventional column, rudder, and power controls. Control feel at the column and rudder pedals is provided by springs which can be ground adjusted for changing the gradients. The current values for linear force gradients, break-out force, and travel are as follows:

TABLE A-1

	Force Gradient, lb/in.	Break out, lb	Travel, inch
Roll column	1.0	0.5	±3.6
Rudder pedal	30.1	1.5	±2.0
Pitch column	4.0	0.5	3.0 fwd; 4.9 aft

Special controls are provided to ensure safety during this potentially hazardous landing research flight operation. The safety pilot can disengage or override the evaluation pilot by a disconnect switch on the control wheel in case of a malfunction or unsafe condition. Manual override is possible for all the hydraulic servo actuators, and system failures are indicated by warning lights.

APPENDIX B

SIDE FORCE AUTHORITY

In order to determine the authority of the side-force surfaces, the following flight tests were performed:

- Flight calibration of the sideslip (β) vane
- Determination of stability derivatives of basic Navion with side-force surfaces held at neutral position
- Steady sideslip configuration flown with side-force surfaces held at a variety of angles

Flight Calibration of β Vane

Two β vanes were installed; one was mounted on the boom extending in the spanwise direction from the tip of the starboard wing, while the other vane was on the boom extending in the chordwise direction in front of the wing tip. A simple cockpit sighting aid which could be aligned with the ground track permitted the angular difference between track and airplane longitudinal axis to be determined. The airplane was first flown in straight-and-level flight over a straight section of railroad track and the pointer of the tracking aid zeroed. The airplane was aligned with the railroad-defined ground track, so that the angle by which the pointer moved indicated the true angle of sideslip. The two β-vane readings were recorded by telemetry.

The experiment checked correspondence with true β, and it verified that the β-vane measurement is not affected by the wake of the side-force surfaces when deflected at various angles.

Further, the spanwise-mounted β vane showed approximately one-to-one correspondence with the readings obtained by the tracker. (Fig. B-1). Since this vane is close to the extended line of the c.g. of the airplane, the need for yaw rate correction is eliminated.

Stability Derivatives of the Basic Navion

Installation of the side-force surfaces caused some changes in the stability derivatives of the basic Navion. To determine the effectiveness of the side-force surfaces ($Y_{\delta y}$) and to facilitate the future simulation of the STOL configurations, it was necessary to obtain the stability derivatives of the Navion with the side-force surfaces held fixed at zero angle. An analog matching procedure was used, whereby the response of the actual airplane to that of the analog simulated model is matched by feeding the airplane control input to the computer model by telemetry. The details of the analog matching method are given in Reference 11. The resulting lateral-directional stability derivatives are given in Table B-2.

Steady Sideslip Experiment

The governing lateral-directional equations of motion for the Navion, with side-force surfaces, may be written (in stability axes) as follows:

$$(s+Y_v)\,\Delta v + V\Delta r - g\Delta\phi = Y_{\delta r}\Delta\delta r + Y_{\delta y}\Delta\delta y$$

$$-L_v\Delta v - L_r\Delta r + (s^2 - L_p s)\Delta\phi = L_{\delta a}\Delta\delta a + L_{\delta r}\Delta\delta r + L_{\delta y}\Delta\delta y \qquad (B1)$$

$$-N_v\Delta v + (s - N_r)\Delta r - N_p s\,\Delta\phi = N_{\delta r}\Delta\delta r + N_{\delta a}\Delta\delta a + N_{\delta y}\Delta\delta y$$

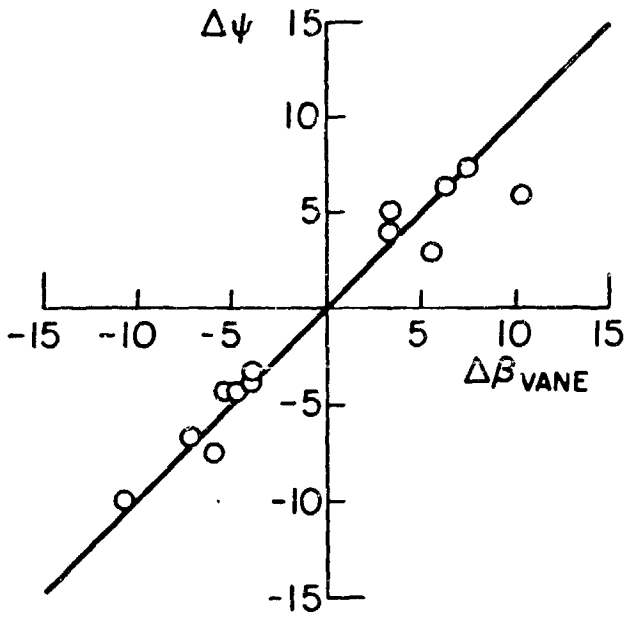

Figure B-1. In-Flight Vane Calibration.

Table B-1

VRA Lateral-Directional Model for 75-kt Airspeed

(Angles in radians, control deflections in inches)

$N_r = -0.685$	$L_r = 1.6$	$Y_\beta/V = -0.315$
$N_\beta = 3.0$	$L_\beta = -6.096$	$g/V = 0.254$
$N_p = -0.199$	$L_p = -4.6$	$Y_{\delta y}/V = 0.25$
$N_{\delta a} = -1.09$	$L_{\delta r} = .392$	$N_{\delta y} = 1.54$
$N_{\delta r} = -4.12$	$L_{\delta a} = 11.4$	$Y_{\delta r}/V = -.047$

For the steady sideslip case, the side-force equation is reduced to

$$\frac{Y_\beta}{V}\Delta\beta + \frac{g}{V}\Delta\phi = \frac{-Y_{\delta y}}{V}\Delta\delta y - \frac{Y_{\delta r}}{V}\Delta\delta r \qquad \text{(B2)}$$

Differentiating with respect to β yields

$$\frac{Y_\beta}{V} + \frac{g}{V}(\partial\phi/\partial\beta) = -\frac{Y_{\delta y}}{V}(\partial\delta y/\partial\beta) - \frac{Y_{\delta r}}{V}(\partial\delta r/\partial\beta)$$

or

$$\frac{Y_{\delta y}}{V} = -\frac{Y_\beta}{V} - \frac{g}{V}\frac{(\partial\phi/\partial\beta)}{(\partial\delta y/\partial\beta)} - \frac{Y_{\delta r}}{V}\frac{(\partial\delta r/\partial\beta)}{(\partial\delta y/\partial\beta)} \qquad \text{(B3)}$$

For Special Case I, $\phi = 0$, and

$$\frac{Y_{\delta y}}{V} = -Y_\beta - \frac{Y_{\delta r}}{V}\frac{(\partial\delta r/\partial\beta)}{(\partial\delta y/\partial\beta)} \qquad \text{(B4)}$$

For Special Case II, $\delta_r = 0$, and

$$\frac{Y_{\delta y}}{V} = -Y_\beta - \frac{g}{V}\frac{(\partial\phi/\partial\beta)}{(\partial\delta y/\partial\beta)} \qquad \text{(B5)}$$

For each setting of the side-force surfaces, the airplane was flown in steady sideslips in both positive and negative directions, and the following data were recorded by telemetry: bank angle (ϕ), sideslip angle (β), rudder surface deflection (δr), aileron surface deflection (δa) and side-force surface deflection (δy). The results are shown in Figures B-2 and B-3 in the form of δr vs. β and ϕ vs. β. The side-force derivative for the side-force surface, $Y_{\delta y}$, is calculated using these figures and the values of the stability derivatives Y_β

and $Y_{\delta r}$ obtained from the analog matching.

The slopes $(\partial\delta r/\partial\beta)$ and $(\partial\delta y/\partial\beta)$ for $\phi = 0$ (Case I), obtained by cross plots of Figures B-2 and B-3, are shown as Figures B-4 and B-5 respectively. Using these, Eq. (B4) yields

$$Y_{\delta y}/V = 0.253 \text{ sec}^{-1} \text{ rad}^{-1}.$$

The required slopes $(\partial\phi/\partial\beta)$ and $(\partial\delta y/\partial\beta)$ for $\delta r = 0$ (Case II) are similarly obtained (Figures B-6 and B-7). Equation (B5) gives

$$Y_{\delta y}/V = 0.248 \text{ rad}^{-1} \text{ sec}^{-1}.$$

Since the two values of $Y_{\delta y}$ obtained in Case I and II are nearly equal, an average value of $Y_{\delta y} = 0.25 \text{ rad}^{-1} \text{ sec}^{-1}$ was selected.

As may be seen from the figures, the sideslip behavior is fairly linear except for the case of δr vs. β for large values of δr. This is believed to be due to an increase in rudder effectiveness for large deflections, evidence of which was noted in the full-scale wind tunnel test of the Navion reported in Ref. 6. Hence, at large rudder deflections, relatively small increments in rudder deflection are needed to balance the airplane in progressively larger steady sideslip conditions, producing the behavior observed in Fig. B-2. However, the nonlinearity is observed for negative (right) deflection only, and no completely satisfactory explanation has been found for this asymmetric behavior. The nonlinearity generally goes unnoticed by evaluation pilots since they are either operating with small sideslip excursions about a trim point, or are commanding rather large dynamic motions such as a decrab.

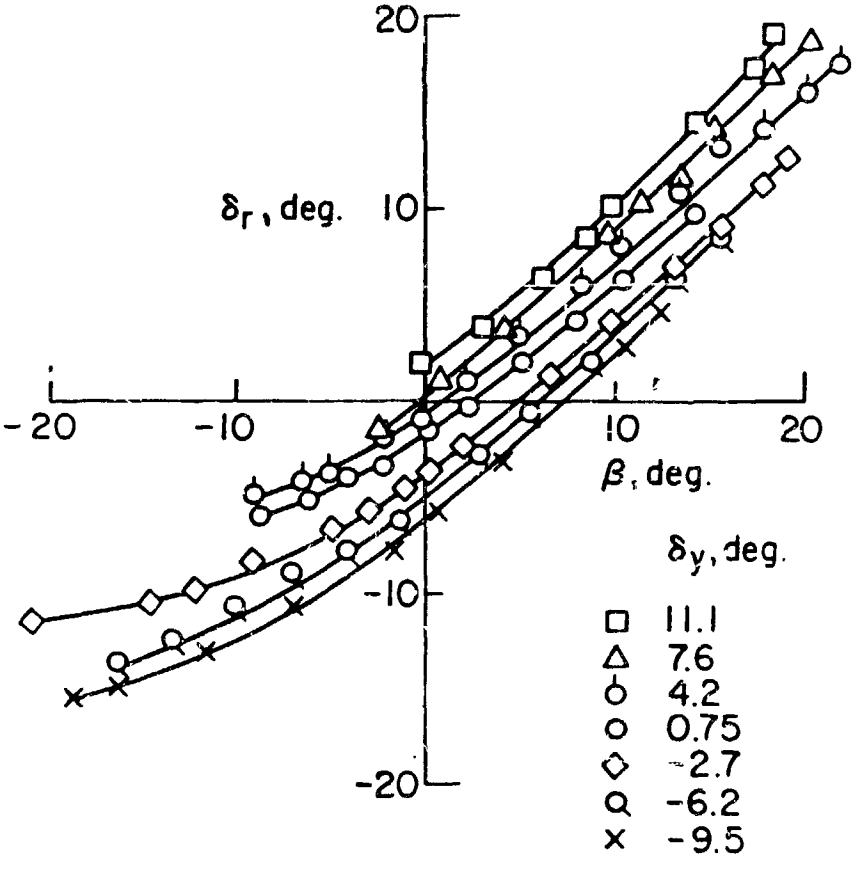

Figure B-2. Flight Calibration, Rudder vs Sideslip.

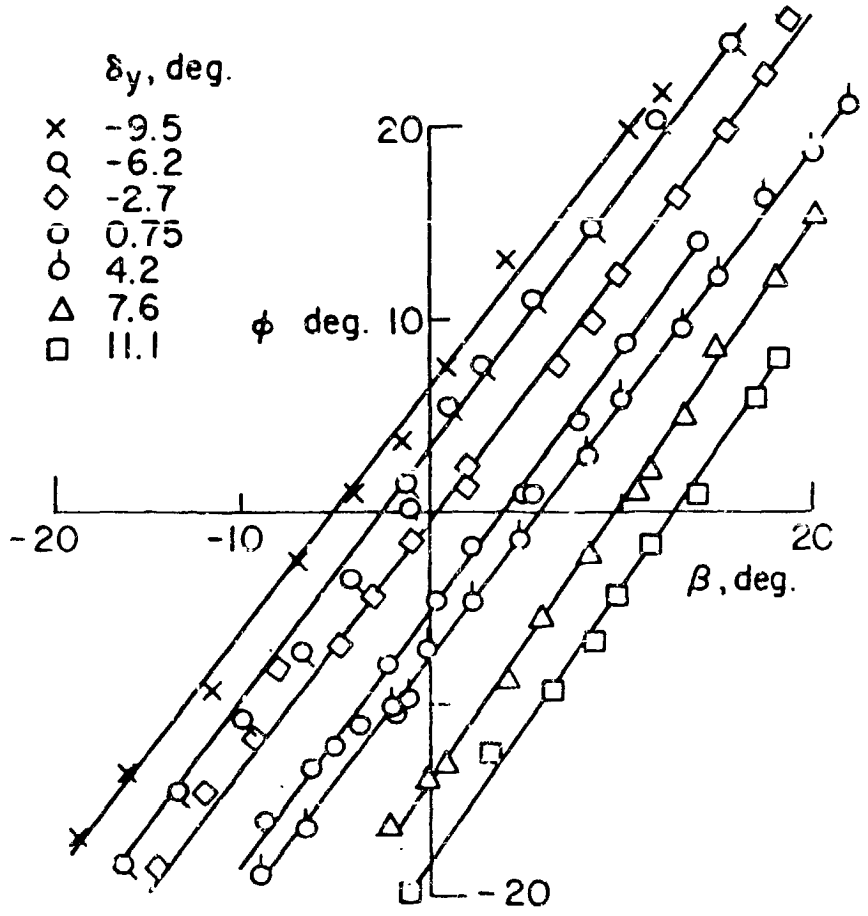

Figure B-3. Flight Calibration, Bank Angle vs Sideslip.

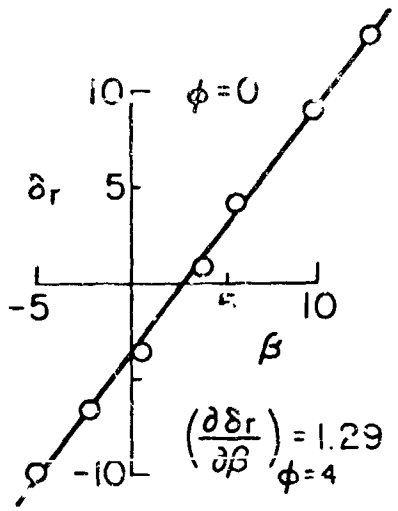

Figure B-4. Wings Level, Rudder vs Sideslip.

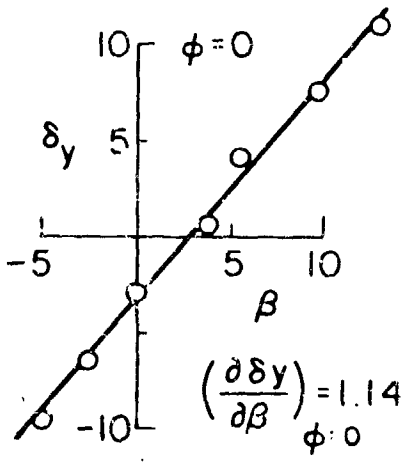

Figure B-5. Wings Level, Side Force Surface vs Sideslip.

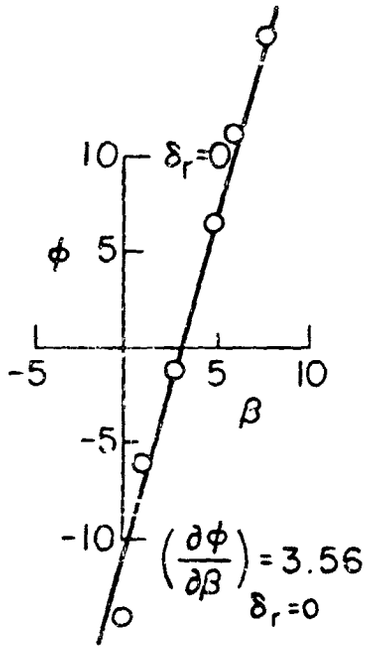

Figure B-6. Neutral Rudder, Bank Angle vs Sideslip.

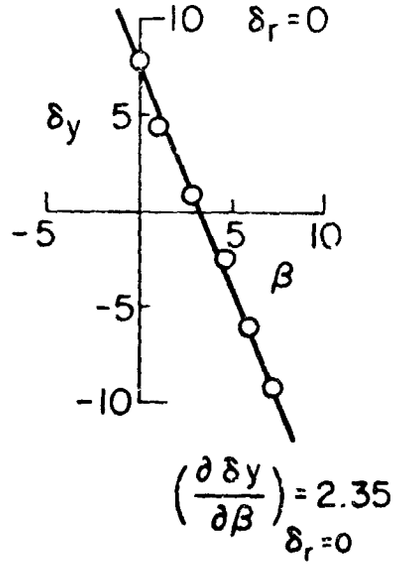

Figure B-7. Neutral Rudder, Side Force Surface vs Sideslip.

REFERENCES

1. Anon. "V/STOL Handling Qualities Criteria. I - Criteria and Discussion", AGARD Report No. 577.

2. Innis, R. C., Holzhauser, C. A., and Quigley, H. C., "Airworthiness Considerations for STOL Aircraft", NASA TN D-5594, January 1970.

3. Doetsch, K. H., Jr., Gould, D. G., and McGregor, D. M., "A Flight Investigation of Lateral-Directional Handling Qualities for V/STOL Aircraft in Low Speed Maneuvering Flight", National Research Council of Canada, LTR-FR-12, August 1969.

4. Anon. "A Flight Simulator Study of STOL Transport Directional Control Characteristics", DOT FA70WA-2395: NDC-J5135 Douglas Aircraft Company, April 1971.

5. Wasserman, R., Eckhart, F. F., and Ledder, H. J., "In-Flight Investigation of an Unaugmented Class III Airplane in the Landing Approach Task: Phase I - Lateral-Directional Study", AFFDL-TR-71-164, Vol. I, January 1972.

6. Smith, R. E., Lebacqz, J. V., and Reford, R. C., "Flight Investigation of Lateral-Directional Flying Qualities and Control Power Requirements for STOL Landing Approach Using the X-22A Aircraft, Volume I: Technical Results", AK-5130-F-1 (Vol. 1), June 1973.

7. Franklin, J. A., "Turbulence and Lateral-Directional Flying Qualities", NASA CR-1718, Princeton University Report No. 890, April 1971.

8. Franklin, J. A., "Turbulence and Longitudinal Flying Qualities", NASA CR-1821, July 1971.

9. Chalk, C. R., Neal, T. P., Harms, T. M., Pritchard, F. E., and Woodcock, R. J., "Background Information and User Guide for MIL-F-8785-B(ASG), Military Specification - Flying Qualities for Piloted Airplanes", AFFDL-TR-69-72, August 1969.

10. Hall, G. W., and Boothe, E. M., "An In-Flight Investigation of Lateral-Directional Dynamics for the Landing Approach", AFFDL-TR-70-145, October 1970.

11. Seckel, E., Miller, G. E., and Nixon, W. B., "Lateral-Directional Flying Qualities for the Power Approach", Princeton University Report No. 727, September 1966.

12. Seckel, E., Stability and Control of Airplanes and Helicopters, Academic Press, 1964.